HHS Public Access

Author manuscript

Neuroscience. Author manuscript; available in PMC 2016 September 10.

Published in final edited form as:

Neuroscience. 2015 September 10; 303: 189–199. doi:10.1016/j.neuroscience.2015.06.050.

COGNITIVE IMPAIRMENT AND MORPHOLOGICAL CHANGES IN THE DORSAL HIPPOCAMPUS OF VERY OLD FEMALE RATS

Gustavo R. Morel[a], **Tomás Andersen**[a], **Joaquín Pardo**[a], **Gustavo O. Zuccolilli**[b], **Vanina L. Cambiaggi**[b], **Claudia B. Hereñú**[a,1], and **Rodolfo G. Goya**[a,1]

[a]INIBIOLP-Histology B -Pathology B, School of Medicine, National University of La Plata. La Plata city, Argentina

[b]Institute of Anatomy, School of Veterinary Sciences, National University of La Plata. La Plata city, Argentina

Abstract

The hippocampus, a medial temporal lobe structure necessary for the formation of spatial memory, is particularly affected by both normal and pathologic aging. In previous studies, we observed a significant age-related increase in dopaminergic neuron loss in the hypothalamus and the substantia nigra of female rats, which becomes more conspicuous at extreme ages. Here, we extend our studies by assessing spatial memory 4–6 months old (young), 26 months old (old) and 29–32 months old (senile) Sprague–Dawley female rats as well as the age-related histopathological changes in their dorsal hippocampus. Age changes in spatial memory performance were assessed with a modified version of the Barnes maze test. We employed two probe trials (PT), one and five days after training, respectively, in order to evaluate learning ability as well as short-term and longer-term spatial memory retention. A set of relevant hippocampal cell markers was also quantitated in the animals by means of an unbiased stereological approach. The results revealed that old rats perform better than senile rats in acquisition trials and young rats perform better than both aging groups. However, during short-term PT both aging groups showed a preserved spatial memory while in longer-term PT, spatial memory showed deterioration in both aged groups. Morphological analysis showed a marked decrease (94–97%) in doublecortin neuron number in the dentate gyrus in both aged groups and a reduction in glial fibrillary acidic protein-positive cell number in the stratum radiatum of aging rats. Astroglial process length and branching complexity decreased in the aged rats. We conclude that while target-seeking activity and learning ability decrease in aged females, spatial memory only declines in the longer-term tests. The reduction in neuroblast number and astroglial arborescence complexity in the dorsal hippocampus are likely to play a role in the cognitive deficits of aging rats.

Corresponding author: Rodolfo G. Goya, INIBIOLP, School of Medicine, UNLP, Calles 60 y 120, 1900 La Plata, Argentina, goya@isis.unlp.edu.ar, Tel. 54-221-425 6735.

[1]These two authors contributed equally to this work.

The hippocampus, a medial temporal lobe structure necessary for the formation of spatial memory, is particularly affected by both normal and pathologic aging impairment (Scoville and Milner, 1957; Corkin et al., 1997; Smith et al., 1999; Stefanacci et al., 2000).

In rats as in humans, learning and memory performance decline with age which makes this rodent species a suitable model to evaluate therapeutic strategies of potential clinical value for restoring age-related cognitive deficits. In previous studies we have reported that hypothalamic or intracerebroventricular insulin-like growth factor-I (IGF-I) gene therapy is able to reverse or at least attenuate the lactotrophic, reproductive and motor derangements of aging female rats (Hereñu et al., 2007; Rodriguez et al., 2013; Nishida et al., 2011), and are now interested in assessing the restorative potential of this intervention on the spatial memory performance of aging female rats. In most rodent studies, spatial memory has been assessed using the Morris Water Maze (MWM, Morris, 1984) for which a considerable performance database is available both for rats and mice. Most rat studies on the impact of aging on spatial memory have been performed in males (some relevant studies are: Barnes et al., 1980; Frick et al., 1995; Barrett et al., 2009; Bizon et al., 2009; McQuail and Nicolle, 2015), a fact that makes it difficult to establish eventual sex-related differences in the impact of aging on cognitive performance. A potential disadvantage of the MWM in aging studies is that it requires a substantial degree of physical fitness. This has led some investigators to prefer the less physically demanding Barnes maze (Barnes, 1979), especially for aged rats. In both tests, rats learn to use spatial cues to guide them to a hidden platform or tunnel. While the MWM involves immersion in water, a stimulus that provokes considerable corticosterone and corticotropin release (Sternberg et al., 1992), in the Barnes maze animals are placed on an open, unprotected circular platform for them to walk in search of the escape tunnel. Comparison between the Barnes maze and MWM in mice has shown that the latter induces higher circulating corticosterone concentration than the former and that serum corticosterone levels show an inverse correlation with the performance of the animals in the MWM but not in the Barnes maze (Harrison et al., 2009). Furthermore, even at the tepid temperatures typically used in MWM studies, swim stress also causes sympathetic activation and peripheral adrenaline release, especially in aged rats (Mabry et al., 1995).

In order to generate a reference framework for future therapeutic investigations in female rats, in the present study we undertook to characterize the changes in spatial memory in old and very old (senescent) females using a modified version of the Barnes maze so that nonspecific exploration and target-seeking activity as well as the ability for acquisition and retention of spatial information can be compared in the different age groups. A set of relevant hippocampal cell markers was also quantitated in the animals by means of an unbiased stereological approach.

1. EXPERIMENTAL PROCEDURES

1.1 Animals

Forty two young (4–6 mo.), twenty old (26 mo.) and thirty seven senile (29–32 mo.) female Sprague-Dawley (SD) rats weighing 199±1, 271±5 and 267±5 g, respectively were used. Animals were housed in a temperature-controlled room (22 ± 2°C) on a 12:12 h light/dark cycle. Food and water were available *ad libitum*. All experiments with animals were

performed in accordance to the Animal Welfare Guidelines of NIH (INIBIOLP's Animal Welfare Assurance No A5647-01).

1.2 Spatial memory assessment

The modified Barnes maze protocol used in this study was based in part on a previously reported procedure (Vargas-Lopez et al., 2011). It consists of an elevated (108 cm to the floor) black acrylic circular platform, 122 cm in diameter, containing twenty holes around the periphery. The holes are of uniform diameter (10 cm) and appearance, but only one hole is connected to a black escape box (tunnel). The escape box is 38.7 cm long × 12.1 cm wide × 14.2 cm in depth and it is removable. A white squared starting chamber (an opaque, 20 cm × 30 cm long, and 15 cm high, open-ended chamber) is used to place the rats on the platform. Four proximal visual cues are placed in the room, 50 cm away from the circular platform. The escape hole was numbered as hole 0 for graphical normalized representation purposes, the remaining holes being numbered 1 to 10 clockwise, and −1 to −9 counterclockwise (Fig. 1). Hole 0 remained in a fixed position, relative to the cues in order to avoid randomization of the relative position of the escape box. During the tests the platform was rotated daily. A 90-dB white-noise generator and a white-light 500 W bulb provided the escape stimulus from the platform. We used an abbreviated protocol based on three days of acquisition trials (AT), followed by two probe trials (PT) (1 and 5 days after training) to assess recent and longer-term spatial memory retention. An AT consists of placing a rat in the starting chamber for 30 s, the chamber is then raised, and the aversive stimuli (bright light and high pitch noise) are switched on and the rat is allowed to freely explore the maze for 120 s. Probe trials are defined as trials where the escape box has been removed, their purpose being to assess the latency to explore the empty escape hole and the error frequency. After the starting chamber is raised, the rat is given 120 s to explore and the number of explorations per hole is recorded. On the day before the first trial (experimental day 0), rats underwent a habituation routine to let them get acquainted with the platform and the escape box. Once AT started, rats were tested (120 s per trial) with the escape box, two times per day for 3 consecutive days (experimental day 1 to 3). On day 4, rats were submitted to a first probe trial (PT1) during 120 s without escape box, followed by a 120-second reinforcement trial with the escape box in place. Afterwards, rats had a 4-day rest (days 5, 6, 7 and 8) and on day 9 they were submitted to a second probe trial (PT2). In order to eliminate olfactive clues from the maze and the boxes, the surfaces were cleaned with 10% ethylic alcohol solution, after each trial.

The behavioral performances were recorded using a computer-linked video camera mounted 110 cm above the platform. The video-recorded performances of the subjects were measured using the Kinovea v0.7.6 (http://www.kinovea.org) and Image Pro Plus v5.1 (Media Cybernetics Inc., Silver Spring, MD) software. The behavioral parameters assessed were as follows.

a. **Escape box latency:** time (in s) spent by an animal since its release from the start chamber until it enters the escape box (during an AT) or until the first exploration of the escape hole (during a PT).

b. **Non-goal hole exploration:** number of explorations of holes different from the escape one. Each exploration of an incorrect hole is counted as an error, provided that the rat lowers its nose below the plane of the table surface.

c. **Hole exploration frequency in the goal sector (GS):** the sum of the number of explorations for holes −1, 0, and 1 divided by 3, during a PT.

d. **Hole exploration frequency in the nongoal sector (NGS):** the sum of explorations of the 17 nongoal holes (i.e., all except holes −1, 0, +1) divided by 17, in a single PT.

e. **Goal Sector Preference:** ratio between GS explorations per hole and NGS explorations per hole. Provides an index of the accuracy with which rats of the same age group remember the GS. Unlike **hole exploration frequency**, this index is independent from the target-seeking activity level of the animals in a given age group.

f. **Total exploratory activity:** the sum of all explorations of a rat in the first AT. This parameter represents the nonspecific exploratory activity of the rats (before they become aware of the presence of an escape box).

g. **Target-seeking activity:** the sum of explorations for all holes in a PT, divided by 20 (ie. mean explorations per hole)

h. **Path length:** distance (in cm) covered by an animal during a given trial, estimated on the basis of reconstructing the route using Image Pro Plus v5.1 software (every 2 s the position of the body center of the rat was followed by manual track object tool in order to reconstruct the route).

i. **Mean velocity:** path length divided by escape box latency (in cm/s). Path length was divided by trial duration during acquisition and probe trials. This measurement does not discriminate between activity and inactivity periods. Path length and mean velocity are a reference parameter for locomotion performance.

Behavioral measurements per trial were grouped for later repeated-measures intra-group comparisons. Significance levels were set at $p < 0.05$.

1.3 Brain processing

Animals were placed under deep anesthesia and perfused with phosphate buffered para-formaldehyde 4%, (pH 7.4) fixative. The brains were rapidly removed and stored in para-formaldehyde 4%, (pH 7.4) overnight (4 °C). Finally, brains were maintained in cryopreservative solution at −20 °C until use. For immunohistochemical assessment, brains were cut coronally in 40 μm-thick sections with a vibratome (Leica).

1.4 Nissl stain

In order to quantify the total number of neurons in the dorsal hippocampus, Nissl staining was performed on brain sections prepared using the same fixation and cutting protocol described for immunohistochemical procedures (see below). Sections were thoroughly rinsed with PBS, put on gelatin-treated slides and air-dried overnight. Then, slides were

briefly washed in distilled water and then immersed in a 0.5% cresyl violet solution at 37°C for 10 minutes. Afterwards, they were washed rapidly in distilled water and dehydrated through a series of graded ethanol (95 % 2 X 30 min and 100% 2 × 5 min each) and cleared in xylene (2 × 5 min each). Slides were coverslipped using Vectamount (Vector Labs, Inc., Burlingame, CA).

1.5 Immunohistochemistry

All immunohistochemical techniques were performed on free-floating sections. For each animal, separate sets of sections were immunohistochemically processed using either an anti-glial fibrillary acidic protein (GFAP) monoclonal antibody 1:500 (G3893, Sigma, Saint Louis, Missouri) or an anti-doublecortin (DCX) goat polyclonal antibody 1:250 (c-18, Santa Cruz Biotech., Dallas, Texas).

For detection, the Vectastain® Universal ABC kit (Vector Labs., Inc., Burlingame, CA, USA) employing 3, 3-diamino benzidinetretrahydro-chloride (DAB) as chromogen, was used. Briefly, after overnight incubation at 4°C with the primary antibody, sections were incubated with biotinylated horse anti-mouse antiserum (1:300, BA-2000, Vector Labs.) or horse anti-goat antiserum (1:300, BA-9500, Vector Labs), as appropriate, for 120 min, rinsed and incubated with avidin-biotin-peroxidase complex (1:500, PK-6100, Vector ABC Elite Kit) for 90 min and then incubated with DAB. Sections were dehydrated, mounted with Vectamount (Vector) and used for image analysis.

1.6 Image Analysis

In each hippocampal block, one every six serial sections was selected in order to obtain a set of non-contiguous serial sections spanning the dorsal hippocampus. Typically, a whole dorsal hippocampus comprises about 66 coronal sections, thus yielding six sets of non-contiguous serial sections (240 μm apart). The number of cells was assessed in the dorsal hippocampus which is located between coordinates −2.8 mm to −4.5mm from the bregma (Paxinos and Watson, 1998) using an Olympus BX-51 microscope, at 500X magnification, attached to an Olympus DP70 CCD video camera (Tokyo, Japan). Cells were counted in 6 anatomically matched sections per animal. The total number o cells were estimated using a modified version of the optical disector method (West, 1993). Individual estimates of the total bilateral neuron number (N) for each region were calculated according to the following formula: $N = RQ\Sigma \cdot 1/ssf \cdot 1/asf \cdot 1/tsf$, where $RQ\Sigma$ is the sum of counted neurons, ssf is the section sampling fraction, asf is the area sampling fraction, and tsf is the thickness sampling fraction. Cells in the uppermost focal plane and/or intersecting the exclusion boundaries of the counting frame were not counted. In all cases, ssf was equal to 1/6 and tsf was equal to 1.

1.7 Nissl stained sections

The total number of pyramidal cells in the CA1 region on Nissl-stained sections was assessed using counting frames measuring 20μm × 20μm at 500X magnification. The volume of the striatum radiatum and hilus was measured based on the Cavalieri principle following the formula: $V = t \times \Sigma Ai$, where t is the distance between sections and ΣAi

represents the sum of areas of each section. Random sampling was done using a 100 μm × 100 μm grid point distance.

1.8 Neuroblast analysis

Neuroblast doublecortin positive {DCX(+) cells} number was assessed using a modified optical fractionator technique (West, 1993) in which we did not use guard zones, making the height of the counting frame equal to section thickness. The top plane was used as the exclusion plane. Due to the low numbers of DCX neurons, the entire subgranular zone (SGZ) and granular cell layer (GCL) sections were used as the counting frame, making the asf = 1. The ssf was 1/6. Estimates were based on counting DCX(+) cell bodies as they came into focus. N= 6 animals per group.

1.9 Astroglial cells

The number of GFAP(+) cells was assessed in the striatum radiatum (beneath the CA1 region) and hilus of the dorsal hippocampus. The number of specimens (N) was 5,6,5 for the Y, O and S groups, resepectively. A counting frame corresponding to 50 μm × 50 μm was employed. Additionally, the area of GFAP(+) cells was determined in the striatum radiatum. A minimum of 30 GFAP(+) cells per region were randomly chosen and captured in each hippocampus under 500X magnification. Only those cells showing completely developed processes and relatively isolated from neighboring cells were selected for the analysis. Cell area was measured using histogram based segmentation with Image Pro Plus software v5.1, while process numbers and length were drawn on a printed image and scanned with a Hewlett-Packard Scanjet G2410 scanner and then scaled up and analyzed with NIH software ImageJ running the Sholl Analysis Plugin v1.0. This technique (Sholl, 1953) consists of superimposing a grid with concentric rings or shells distributed at equal distances **d** centered on the soma of a cell. The number of process intersections **i** per shell was computed and branching complexity evaluated. The length of the processes was estimated by the sum of the products of **d** by **i** for each ring. Branching complexity and process length analysis could not be done for DCX cells due to insufficient number of cells to achieve statistical validity, particularly in the aged rats.

1.10 Statistical analysis

Data were compiled and analyzed with the Sigma Plot v. 11 software (San Jose, CA). Comparisons between groups were made using repeated-measures ANOVA for the acquisition and probe trials, whereas factorial ANOVA was used for stereological data. Behavioral and stereological data are presented as mean ± SEM. Holm-Sidak and Tukey's post-hoc tests were used where appropriate. Criteria for significant differences were set at the 95% probability level.

RESULTS

2.1 Cognitive changes

2.1.1 Latency to escape box—After AT1, escape hole latency fell rapidly in young and more gradually in old rats, but remained virtually unchanged throughout the 6 AT in the senile animals (Fig 2, **left upper panel;** two-way RM ANOVA $F_{2,5}$ (age)=28.793; P<0.001;

$F_{2,5}$ (trial)=15.987; P<0.001). From AT 2 to 4, young animals showed a better performance in the time to reaching the escape hole than both aging groups but at AT 5 and 6 the old rats caught up with their young counterparts.

In PT1 (1 day after ATs), escape hole latency was significantly longer in senile than in young rats whereas young and old animals performed similarly (Fig 2, **right upper panel;** two-way RM ANOVA $F_{2,1}$ (age)=27.374; P<0.001; $F_{2,1}$ (trial)=11.072; P=0.001). In PT2 (5 days after ATs), escape hole latency was significantly longer in both old and senile than in young rats. The old and senile rats that froze when placed on the platform were removed from the study.

2.1.2 Errors to escape box—During the AT series, nongoal hole exploration (i.e., errors) numbers decreased significantly from AT1 to AT2 in the young rats, remaining constant afterwards. This reduction in error frequency was also significant but less consistent in old rats. Only in AT4, differences between young and aged rats became significant (Fig. 2, **left lower panel,** two-way RM ANOVA $F_{2,5}$ (age)=5.435; P=0.06; $F_{2,5}$ (trial)=3.988; P=0.002). In PT2 but not in PT1, old and senile animals showed an increase in the number of errors as compared to young rats (Fig. 2, **right lower panel;** two-way RM ANOVA $F_{1,2}$(age)=6.256; P<0.003; $F_{1,2}$ (trial)=0.097; NS). This increase was significant in old, but was only a trend in senile rats (P=0.061)

2.1.3 Hole exploration frequency—Hole exploration frequency showed a bell-shaped distribution around hole 0 in PT1 in all age groups (Fig. 3, **middle and lower panels**). However, the shape of the bell was less well-defined as the age of the animals increased, reflecting a progressive age-related deterioration of recent spatial memory. In PT2 hole exploration frequency also showed a bell-shaped distribution around hole# 0, but the shape of the curve was less well-defined than in PT1 particularly for the old and senile groups. In PT2 the curve for senile rats retained little resemblance to a bell.

2.1.4 Goal sector exploration—Young rats showed a significantly higher exploratory activity than aging rats for the GS in both PT1 and PT2, particularly when the GS was taken as hole 0 instead of holes −1, 0 and 1 (Fig. 3, **upper panels,** one-way ANOVA F_2 (age) had a P<0.01 for the 4 plots), whereas the exploratory frequency for the NGS was less affected by age (**data not shown**). Total nonspecific exploratory activity for each age group was {mean ± SEM explorations in AT1 (n= number of rats)}, 3.9±0.5 (n=28), 5.5±0.8 (n=20) and 3.5±0.6 (n=17) for the young, old and senescent groups, respectively and did not differ significantly among age groups. In contrast, target-seeking activity declined with age and was slightly lower in PT2 than PT1 for each age group (Table 1).

The preference of rats to explore the GS versus NGS was chosen as an index dependent of spatial memory but not of target-seeking activity. In PT1, GS preference did not change significantly with age even when the GS was restricted to hole 0. In contrast, GS preference fell significantly with age in PT2, particularly when the GS was defined as hole 0 (Fig. 4).

2.1.5 Path length—From AT1 through AT6 the distance walked to find the target hole diminished in young and old but not in senile rats (Fig. 5, left panel; two-way RM ANOVA

$F_{2,5}$ (age)=7.496; P<0.05; $F_{2,5}$ (trial)=5.990; P<0.001) whereas probe trials revealed no significant differences among the age groups (Fig. 5, **right panel;** two-way RM ANOVA $F_{,2,1}$(age)=1.782; NS; $F_{2,1}$ (trial)=3.449; NS).

2.1.6 Mean velocity—Mean velocity showed a significant although irregular increase throughout the training trials in young animals but remained without significant changes, in both old and senile rats (Fig. 6, **left panel;** two-way RM ANOVA $F_{2,5}$ (age)=19.677; P<0.001; $F_{2,5}$ (trial)=3.091; P<0.02). Mean velocity was comparable in young and old rats but decreased significantly in the senile animals during both PT (Fig. 6, **right panel;** two-way RM ANOVA $F_{2,1}$(age)=4.697; P<0.02; $F_{2,1}$ (trial)=3.584; P= 0.07 (NS)).

2.2. Morphologic age changes in the dorsal hippocampus

A stereological assessment of neurons, migrating neuroblasts and glial cells was performed in the dorsal hippocampus of young and aged rats. Nissl staining revealed no differences among the three age groups in the number of neurons in the CA1 of the **stratum pyramidale**, nor in the volume of stratum radiatum or hilus (Table 2). In contrast, there was a 94% and 97 % reduction in the number of DCX cells (neuroblasts) in the dentate gyrus (DG) of old and senile rats, respectively as compared with the young animals (Fig. 7D; one-way ANOVA; $\mathbf{F_2(age)}$=42.868; P<0.001).

The number of GFAP (astroglial) cells declined progressively with age in the stratum radiatum, showing a 25% ($p < 0.05$) and 28 % ($p < 0.05$) reduction in the old and senile rats, respectively as compared with the young animals (Fig. 7H; one-way ANOVA; F_2=13.375; P<0.006). In contrast, the number of GFAP cells in the hilus region was not significantly affected by age (data not shown). Although no significant age changes were detected in the size of processes in GFAP cells, a significant reduction in length and complexity was found in the stratum radiatum (Fig. 8; one-way ANOVA; F_2=11.469 P<0.001).

3. DISCUSSION

Taken together, our behavioral results showing that spatial memory is impaired in old and senescent SD female rats are qualitatively consistent with the consensus results that have emerged from previous studies in other rat strains based either on the MWM or Barnes maze (Barnes et al., 1980; Frick et al., 1995; Barrett et al., 2009; Bizon et al., 2009; McQuail and Nicolle, 2015). A study in SD female rats of different ages used two performance parameters, errors per day and criterion attainment, to assess Barnes maze performance (Barrett et al., 2009). It was found that the errors per day increased with age which is in line with our results, although we observed a more gradual, age-related increase in the number of errors during the training trials, as did Barnes in Long-Evans male rats (Barnes, 1979). In the above study by Barret et al., the % of rats reaching criterion during the trial period declined with age. Instead of criterion, we measured the latency to escape box during acquisition trials as a learning index and also found a decline of learning ability in the aged females. In a previous study in middle-aged (12 months) SD females, we observed no changes in learning ability or spatial memory as compared with young (2 months) counterparts (Morel et al., unpublished). The MWM probe trial, which measures specifically the spatial component of target-finding, has no counterpart in the Barnes maze, although

more recently, removal of the escape box has been used to assess spatial memory extinction (Vargas-Lopez et al., 2011). By removing the escape box at the end of the training period we introduced the PT in our variant of the test, which enabled us to assess memory-dependent and independent parameters as well as recent (PT1) and longer-term (PT2) retention of spatial memory, whose magnitude is proportional to the inverse of spatial memory extinction. The moderate deterioration in recent (PT1) and longer-term (PT2) spatial memory retention, as assessed by latency to escape hole and number of errors, revealed by our study is in line with PT in MWM studies in young (3 mo) and middle-aged (12 mo) male SD rats where no significant age differences were detected either in platform trials (using swim time and swim distance measures) and in one probe trial measure (percent of swim path spent in the correct quadrant). However, the 12-month-old rats were impaired on the platform crossings measure during the probe trial (Fischer et al., 1992).

Similarly, in another MWM study it was found that 11-month-old Fischer-344 rats are impaired in the platform crossings measure but not in other less challenging PT (Frick et al., 1995). Note that the platform crossings measure is a highly challenging measure because it requires precise localization of the platform. The two above reports indicate the presence of a mild spatial reference memory deficit in rats as young as 11 to 12 months which becomes detectable only in difficult measures of performance. Relative to MWM PT, our PT can be considered slightly less difficult. The distribution profile of hole exploration frequencies in PT1 and PT2 provides a useful index of recent and longer-term spatial memory retention. The sharpness of the bell-shaped curve around hole 0 reflects the accuracy with which rats remember the spatial location of the escape hole in the absence of the tunnel. A similar bell-.shaped distribution of exploratory activity has been reported in 66-day old male Wistar rats in the Barnes maze (Vargas-Lopez et al., 2011). This accuracy deteriorates with age and to a lesser extent, with the time elapsed since the end of the training period. In order to have a more convenient way to quantitate spatial memory retention we calculated the GS exploratory frequency, expressed as the mean number of explorations per each GS hole. This parameter was calculated for a GS consisting of only the escape hole and for a GS consisting of hole −1, 0 & 1, and in the two instances we observed a significant age-related fall in GS exploration frequency, particularly when GS was taken as only the escape hole. At least two components contribute to the magnitude of GS exploration frequency namely, spatial memory retention and target-seeking activity. The lattermainly depends on the motivation to search for the escape hole which our results show to decline with age (Table 1). Since nonspecific exploratory activity did no change with age, it seems that it is the drive to find the escape box what declines with age. While swim speed declines with age in the MWM (Bizon et al., 2009), locomotive activity (mean velocity) in the Barnes maze does not (Frick et al. and Fig 6), which makes it unlikely that physical fitness play a role in the decline of the GS exploratory frequency in the aged rats. *Goal Sector preference,* a parameter not affected by age changes in target-seeking motivation, revealed that recent spatial memory is not significantly affected by age under the mild stress conditions of the Barnes maze. In contrast, longer-term spatial memory, assessed by measuring GS preference, significantly deteriorates with age, particularly when the test requires high accuracy (i.e., single hole GS). It should be pointed out that there are other noncognitive

factors likely to affect GS preference in aged rats. One of them is the decline in visual acuity that occurs in aged rats. Therefore, GS preference in not reflecting purely cognitive abilities.

Several studies have documented that the progressive decline in spatial memory performance in aged rats is associated to, and probably preceded by underlying structural, cellular and molecular changes in the hippocampus, the vast majority of data having been generated in males (Sugaya et al., 1996; Geinisman et al., 2004; Jacobson et al., 2008; Begega et al., 2012; Masser et al., 2014).

In order to find a possible correlation between behavioral performance and morphological changes in the dorsal hippocampus of aged female rats, we performed a stereological assessment of neurons and astroglial cells in two regions vulnerable to aging, namely the CA1 and DG regions. In line with observations in aged males (Rapp and Gallagher, 1996) no significant adult neuron loss was detected in the dorsal hippocampus of our aged females. However, other studies reported hippocampal neuronal loss in aged rats. Thus, *Shetty et al (1999)* found a decreased number of hilar neurons in male 22-mo old Fischer 344 rats. In addition, Azcoitia et al (2005) reported a significant neuronal loss in the dentate hilux of male Wistar rats aged between 22 and 24 month-old, compared with 18 month-old counterparts. This discrepancy could be accounted for by differences in the hippocampal region studied, as we counted in the whole hippocampus, not just in the hilux.

Doublecortin is a cytoskeleton-associated protein involved in structural plasticity (Gleeson et al., 1999) and is widely expressed during central nervous system development, becoming progressively restricted during adulthood, with high expression within regions of persistentneurogenesis (Francis et al., 1999; Nacher et al., 2001). In newly generated neurons, DCX acts in the microtubule cytoskeleton to promote/allow migration and differentiation of immature neurons (Koizumi et al., 2006). Our finding that hippocampal neurogenesis is dramatically reduced in aged female rats is in line with the results from Kuhn et al (1996) who labeled Fischer 344 female rats with BrdU and found that 12- to 27-month-old animals exhibited a significant decline in the density of BrdU-positive cells in the hippocampal granule cell layer as compared with 6-month-old counterparts. In Wistar female rats, Perez Martin et al (2005) observed a significant reduction in the number of BrdU-immunoreactive cells in 22 months old as compared with 14 and 18 months old animals. Furthermore, Rao et al (2006) demonstrated that newly born neurons in the aging DG exhibit diminished dendritic growth when compared with their counterparts in the young DG. The sharp fall in neurogenic potential in the dorsal hippocampus of aged rats is likely to play a role in their spatial memory deficits.

Astrocytes display increasing activation with age, a phenomenon that is disruptive to neuronal function (Rozovsky et al., 2005). In this context, GFAP, an intermediate filament protein, is known to be overexpressed by reactive astroglia. Although the variable changes that we observed in GFAP expression in the dorsal hippocampus of our aged rats are difficult to interpret, it seems reasonable to assume that they are likely to contribute to the overall decline in cognitive function.

The age-related reduction that we observed in the length and complexity of hippocampal astrocytes was a more consistent finding than the changes in GFAP. A reduced branching in aged astrocytes may impair the ability of these glial cells to provide trophic support to neurons. In contrast to the classical synapse paradigm, nowadays it is well accepted that astrocytes play a key role in this process, giving rise to the concept of tripartite synapse (reviewed in Perea et al 2009). Therefore, less branched astrocytes in the aged hippocampus may be less effective to strengthen synapse functioning. Since astrocytes play a relevant role in the metabolism of neurotransmitters by regulating extracellular potassium and glutamate homeostasis (Ota et al 2013), it is also possible that the observed age-related reduction in astrocyte branching adversely affects these parameters.

3.1 Conclusions

We conclude that the Barnes maze is a convenient tool to quantitate the different components of spatial memory in aged rats and is sufficiently sensitive to detect age changes in these components. The aged female SD rat shares, in general terms, cognitive and cellular hippocampal cell deficits with other rat strains and represents a suitable animal model for implementing therapeutic interventions that by boosting hippocampal neurogenesis and revitalizing glial cells and neurons, may restore cognitive function in old individuals.

Acknowledgments

Funding. This work was supported by grant # R01AG029798 from the Fogarty International Center and the National Institute on Aging, NIH, to RGG, grant #PICT11-1273 from the Argentine Agency for the Promotion of Science and Technology to RGG and by grant PIP0597 from the Argentine Research Council (CONICET) to RGG.

The authors are indebted to Ms. Yolanda E. Sosa for technical and editorial assistance. GRM, CBH and RGG are career researchers of CONICET. JP is a recipient of a CONICET doctoral fellowship. TA was recipient of an Interuniversity Council (CIN) undergraduate fellowship and GOZ and VLC are associate professors at the School of Veterinary Sciences, National University of La Plata.

ABBREVIATIONS

AT	Acquisition trial
DG	Dentate gyrus
DH	Dentate hilus
DCX	Doublecourtin
GFAP	Glial Fibrillary Acidic Protein
GS	Goal sector
GCL	Granular cell layer
IGF-I	Insulin-like Growth Factor I
ML	Molecular layer
MWM	Morris WaterMaze
NGS	Non-goal Sector

PT Probe Trial

References

Azcoitia I1, Perez-Martin M, Salazar V, Castillo C, Ariznavarreta C, Garcia-Segura LM, Tresguerres JA. Growth hormone prevents neuronal loss in the aged rat hippocampus. Neurobiol Aging. 2005; 26:697–703. [PubMed: 15708445]

Barnes CA. Memory deficits associated with senescence: a neurophysiological and behavioral study in the rat. J Comp Physiol Psychol. 1979; 93:74–104. [PubMed: 221551]

Barnes CA, Nadel L, Honig WK. Spatial memory deficit in senescent rats. Can J Psychol. 1980; 34:29–39. [PubMed: 7388694]

Barrett GL, Bennie A, Trieu J, Ping S, Tsafoulis C. The chronology of ag related spatial learning impairment in two rat strains, as tested by the Barnes maze. Behav Neurosci. 2009; 123:533–538. [PubMed: 19485559]

Begega A1, Cuesta M, Rubio S, Méndez M, Santín LJ, Arias JL. Functional Networks involved in spatial learning strategies in middle-aged rats. Neurobiol Learn Mem. 2012; 97:346–353. [PubMed: 22406474]

Bizon JL, LaSarge CL, Montgomery KS, McDermott AN, Setlow B, Griffith WH. Spatial reference and working memory across the lifespan of male Fischer 344 rats. Neurobiol Aging. 2009; 30:646–655. [PubMed: 17889407]

Corkin S, Amaral DG, Gonzalez RG, Johnson KA, Hyman BT. H. M'.s medial temporal lobe lesion: findings from magnetic resonance imaging. J Neurosci. 1997; 17:3964–3979. [PubMed: 9133414]

Fischer W, Chen KS, Gage FH, Björklund A. Progressive decline in spatial learning and integrity of forebrain cholinergic neurons in rats during aging. Neurobiol Aging. 1992; 13:9–23. [PubMed: 1311806]

Francis F, Koulakoff A, Boucher D, Chafey P, Schaar B, Vinet MC, Friocourt G, McDonnell N, Reiner O, Kahn A, McConnell SK, Berwald-Netter Y, Denoulet P, Chelly J. Doublecortin is a developmentally regulated, microtubule-associated protein expressed in migrating and differentiating neurons. Neuron. 1999; 23:247–256. [PubMed: 10399932]

Frick KM, Baxter MG, Markowska AL, Olton DS, Price DL. Age-related spatial reference and working memory deficits assessed in the water maze. Neurobiol Aging. 1995; 16:149–160. [PubMed: 7777133]

Geinisman YL, Ganeshina O, Yoshida R, Berry RW, Disterhoft JF, Gallagher M. Aging, spatial learning, and total synapse number in the rat CA1 stratum radiatum. Neurobiol Aging. 2004; 25:407–416. [PubMed: 15123345]

Gleeson JG, Lin PT, Flanagan LA, Walsh CA. Doublecortin is a microtubule associated protein and is expressed widely by migrating neurons. Neuron. 1999; 23:257–271. [PubMed: 10399933]

Harrison FE, Hosseini AH, McDonald MP. Endogenous anxiety and stress responses in water maze and Barnes maze spatial memory tasks. Behav Brain Res. 2009; 198:247–251. [PubMed: 18996418]

Hereñú CB, Cristina C, Rimoldi OJ, Becú-Villalobos D, Cambiaggi V, Portiansky EL, Goya RG. Restorative effect of Insulin-like Growth Factor-I gene therapy in the hypothalamus of senile rats with dopaminergic dysfunction. Gene Ther. 2007; 14:237–245. [PubMed: 16988717]

Jacobson LI, Zhang R, Elliffe D, Chen KF, Mathai S, McCarthy D, Waldvogel H, Guan J. Correlation of cellular changes and spatial memory during aging in rats. Exp Gerontol. 2008; 43:929–438. [PubMed: 18761081]

Koizumi H, Higginbotham H, Poon T, Tanaka T, Brinkman BC, Gleeson JG. Doublecortin maintains bipolar shape and nuclear translocation during migration in the adult forebrain. Nature Neurosci. 2006; 9:779–786. [PubMed: 16699506]

Kuhn HG, Dickinson-Anson H, Gage FH. Neurogenesis in the dentate gyrus of the adult rat: age-related decrease of neuronal progenitor proliferation. J Neurosci. 1996; 16:2027–2033. [PubMed: 8604047]

Mabry TR, Gold PE, McCarty R. Age-related changes in plasma catecholamine responses to acute swim stress. Neurobiol Learn Memory. 1995; 63:260–268.

Masser DR, Bixler GV, Brucklacher RM, Yan H, Giles CB, Wren JD, Sonntag WE, Freeman WM. Hippocampal subregions exhibit both distinct and shared transcriptomic responses to aging and nonneurodegenerative cognitive decline. J Gerontol A Biol Sci Med Sci. 2014; 69:1311–1324. [PubMed: 24994846]

McQuail JA, Nicolle MM. Spatial reference memory in normal aging Fischer 344 × Brown Norway F1 hybrid rats. Neurobiol Aging. 2015; 36:323–333. [PubMed: 25086838]

Morris R. Developments of a water-maze procedure for studying spatial learning in the rat. J Neurosci Meth. 1984; 11:47–60.

Nacher J, Crespo C, McEwen BS. Doublecortin expression in the adult rat telencephalon. Eur J Neurosci. 2001; 14:629–644. [PubMed: 11556888]

Nishida F, Morel GR, Hereñú CB, Schwerdt JI, Goya RG, Portiansky EL. Restorative effect of intracerebroventricular Insulin-like Growth Factor-I gene therapy on motor performance in aging rats. Neuroscience. 2011; 177:195–206. [PubMed: 21241779]

Ota Y, Zanetti AT, Hallock RM. The role of astrocytes in the regulation of synaptic plasticity and memory formation. Neural Plast. 2013; 2013:article ID185463. 11 pages.

Paxinos, G.; Watson, C. The rat brain in stereotaxic coordinates. 4. Academic Press; San Diego, CA: 1998.

Perea G, Navarrete M, Araque A. Tripartite synapses: astrocytes process and control synaptic information. Trends Neurosci. 2009; 32:421–431. [PubMed: 19615761]

Perez-Martin MI, Salazar V, Castillo C, Ariznavarreta C, Azcoitia I, Garcia-Segura LM, Tresguerres JA. Estradiol and soy extract increase the production of new cells in the dentate gyrus of old rats. Exp Gerontol. 2005; 40:450–453. [PubMed: 15885957]

Rao MS, Hattiangady B, Shetty AK. The window and mechanisms of major age-related decline in the production of new neurons within the dentate gyrus of the hippocampus. Aging Cell. 2006; 5:545–558. [PubMed: 17129216]

Rapp PR, Gallagher M. Preserved neuron number in the hippocampus of aged rats with spatial learning deficits. Proc natl Acad Sci USA. 1996; 93:9926–9930. [PubMed: 8790433]

Rodriguez SS, Schwerdt JI, Barbeito CG, Flamini AM, Han Y, Bohn MC, Goya RG. Hypothalamic insulin-like growth factor-I gene therapy prolongs estral cyclicity and protects ovarian structure in middle-aged female rats. Endocrinology. 2013; 154:2166–2173. [PubMed: 23584855]

Rozovsky I, Wei M, Morgan TE, Finch CE. Reversible age impairments in neurite outgrowth by manipulations of astrocytic GFAP. Neurobiol Aging. 2005; 26:705–715. [PubMed: 15708446]

Scoville WB, Milner B. Loss of recent memory after bilateral hippocampal lesions. J of Neurol Neurosurg Psych. 1957; 20:11–21.

Shetty AK, Turner DA. Vulnerability of the dentate gurys to aging and intra-cerebroventricular administration of kainic acid. Exp Neurol. 1999; 158:491–503. [PubMed: 10415155]

Sholl DA. Dendritic organization in the neurons of the visual and motor cortices of the cat. J Anat. 1953; 87:387–406. [PubMed: 13117757]

Smith TD, Calhoun ME, Rapp PR. Circuit and morphological specificity of synaptic change in the aged hippocampal formation. Neurobiol Aging. 1999; 20:357–360. [PubMed: 10588586]

Stefanacci L, Buffalo EA, Schmolck H, Squire LR. Profound amnesia after damage to the medial temporal lobe: a neuroanatomical and neuropsychological profile of patient E. P. J Neurosci. 2000; 20:7024–7036. [PubMed: 10995848]

Sternberg EM, Glowa JR, Smith MA, Calogero AE, Listwak SJ, Aksentijevich S, Chrousos GP, Wilder RL, Gold PW. Corticotropin releasing hormone related behavioral and neuroendocrine responses to stress in Lewis and Fischer rats. Brain Res. 1992; 570:54–60. [PubMed: 1319794]

Sugaya K, Chouinard M, Greene R, Robbins M, Personett D, Kent C, Gallagher M, McKinney M. Molecular indices of neuronal and glial plasticity in the hippocampal formation in a rodent model of age-induced spatial learning impairment. J Neurosci. 1996; 16:3427–3443. [PubMed: 8627377]

Vargas-López V, Lamprea MR, Múnera A. Characterizing spatial extinction in an abbreviated version of the Barnes maze. Behav Proc. 2011; 86:30–38.

West MJ. New stereological methods for counting neurons. Neurobiol Aging. 1993; 14:275–285. [PubMed: 8367009]

HIGHLIGHTS

- Spatial memory and hippocampal histopathology wass assessed in aged female rats.
- There is an age-dependent decline in learning in female rats but not in short-term spatial memory.
- Longer- term spatial memory declined significantly in the aged animals.
- Doublecortin neuron number and astroglial process length and branching complexity decreased in the aged rats.

Figure 1. Barnes Maze design used in the present study

The maze consists of a black acrylic circular platform, 122 cm in diameter, containing twenty holes around the periphery. The holes are of uniform diameter (10 cm) and appearance, but only one hole is connected to a black escape box. An opaque squared starting chamber is used to place the rats on the platform. Four proximal visual cues are located in the room, 50 cm away from the circular platform. The escape hole is numbered as hole 0 for graphical normalized representation purposes, the remaining holes being numbered 1 to 10 clockwise, and −1 to −9 counterclockwise. Hole 0 remains in a fixed position, relative to the cues in order to avoid randomization of the relative position of the escape box.

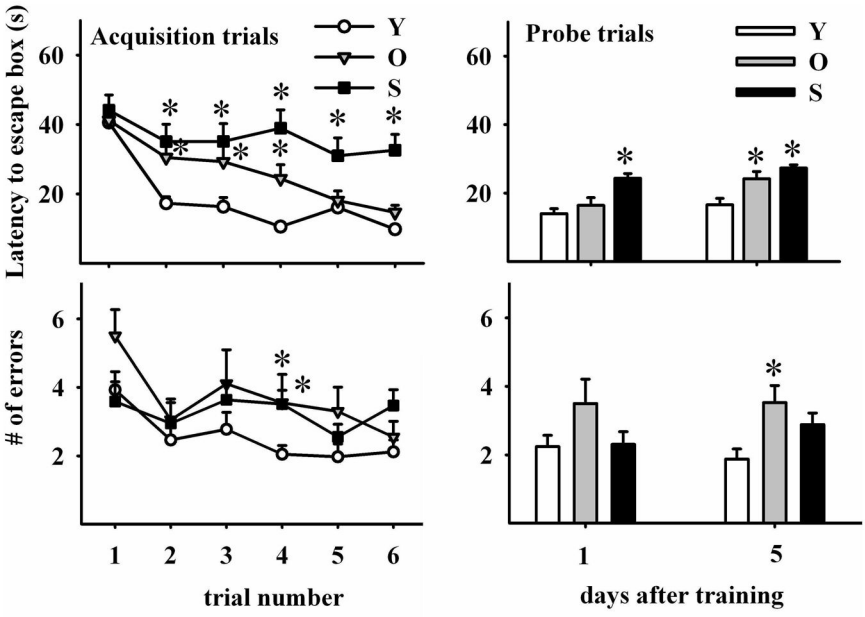

Figure 2. Effect of age on learning and spatial memory retention

Upper panels show escape hole latency throughout training (**upper left panel**) and in probe trials (**upper right panel**). Lower panels show the number of errors during training (**left lower panel**) and probe trials (**right lower panel**). Learning ability was assessed by performing six acquisition trials during three days (2 AT per day). Note that young rats show the greatest overall reduction in primary errors (errors made before the first exploration of hole 0) during acquisition. All data are represented as mean ∀ SEM. Comparisons are made versus the corresponding young data point. *: $P<0.05$; Number of young, old and senescent rats for AT was 30, 20 and 15 and was 42, 20 and 37 for PT, respectively.

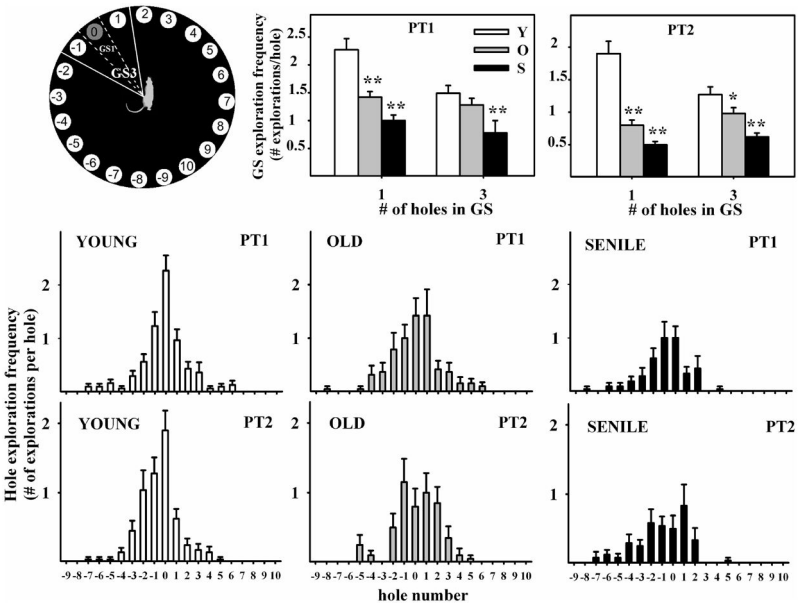

Figure 3. Hole exploration frequency in probe trials

Notice in the **middle and lower panels**, the bell-shaped distribution of frequencies around hole #0 and the age-related deterioration of this bell shape. **Center and right upper panels** show goal sector exploration in young, old and senescent rats. Exploratory activity was measured when GS was taken as only hole #0 (delineated by dashed lines) or when the GS consisted of holes −1, 0 and 1 (delineated by solid lines), as illustrated on the left upper panel. Number of young, old and senescent rats for PT1 was 30, 19 and 21 and for PT2 was 29, 20 and 24, respectively. *P<0.05; **P<0.01; Tukey's post hoc test.

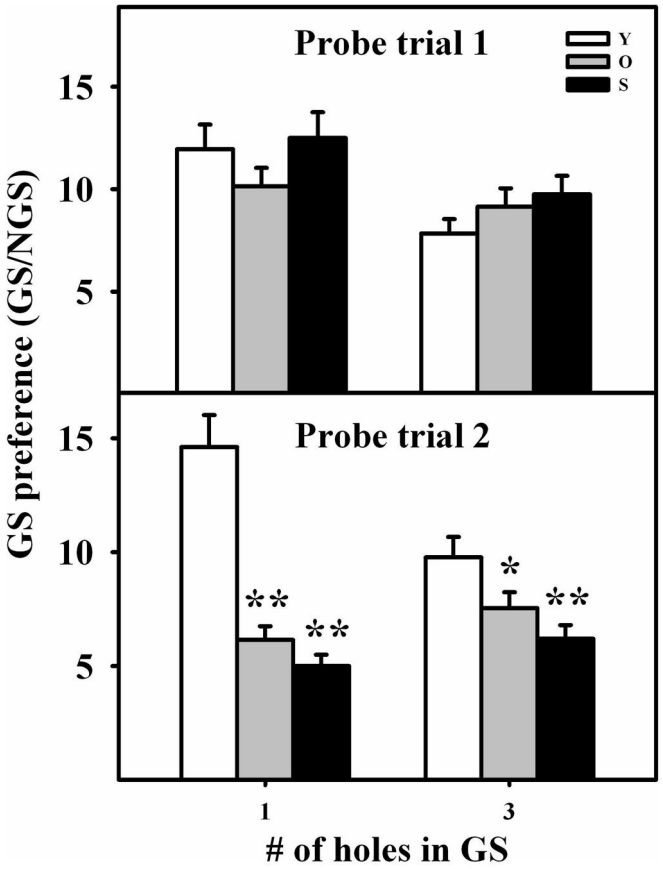

Figure 4. Goal Sector Preference in young, old and senile rats

Columns represent the ratio, GS explorations per hole/NGS explorations per hole, in the different age groups, for GS consisting of either hole# 0 or holes −1,0,1. This ratio provides an index of the accuracy with which rats of the same age group remember a given GS. Notice that this ratio is independent from the target-seeking activity level of rats in a given age group. Statistical comparisons are made versus the young group of each set. *: $P<0.05$; **: $P<0.01$. Number of young, old and senescent rats for PT1 was 30, 19 and 21 and for PT2 was 29, 20 and 24, respectively. Other details are as in Fig. 2.

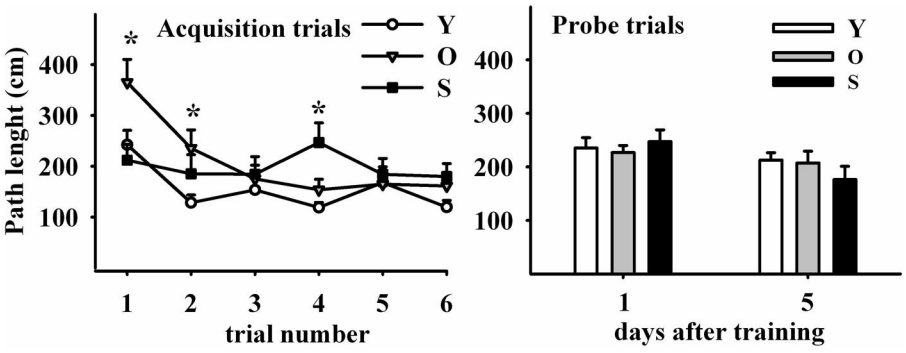

Figure 5. Path length evolution throughout training and probe trials

Left Panel illustrates six acquisition trials during three days (at 2 AT per day). Distance traveled in the maze was progressively reduced in young and old but not in senile rats. **Right Panel** shows path length in two probe trials performed four days apart, in young, old and senile rats. Path length was no different among age groups. N values and other details are as in Fig 2. The Holm-Sidak post hoc test was used for group comparisons

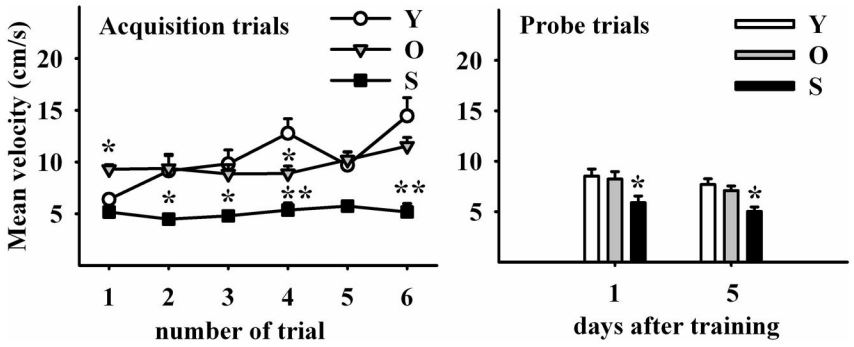

Figure 6. Mean Velocity evolution throughout training

Left Panel illustrates six acquisition trials during three days. Mean velocity in the maze progressively increased in young but not in old and senile rats. Note that old rats began with higher speeds than their young counterparts. **Right Panel** shows mean velocity in two probe trials five days apart. Senile rats showed a significantly lower speed than young and old counterparts in both probe trials. (Holm-Sidak pos-hoc method applied to probe trial 1 and Dunn's Method for probe trial 2). N values and other details are as in Fig 2.

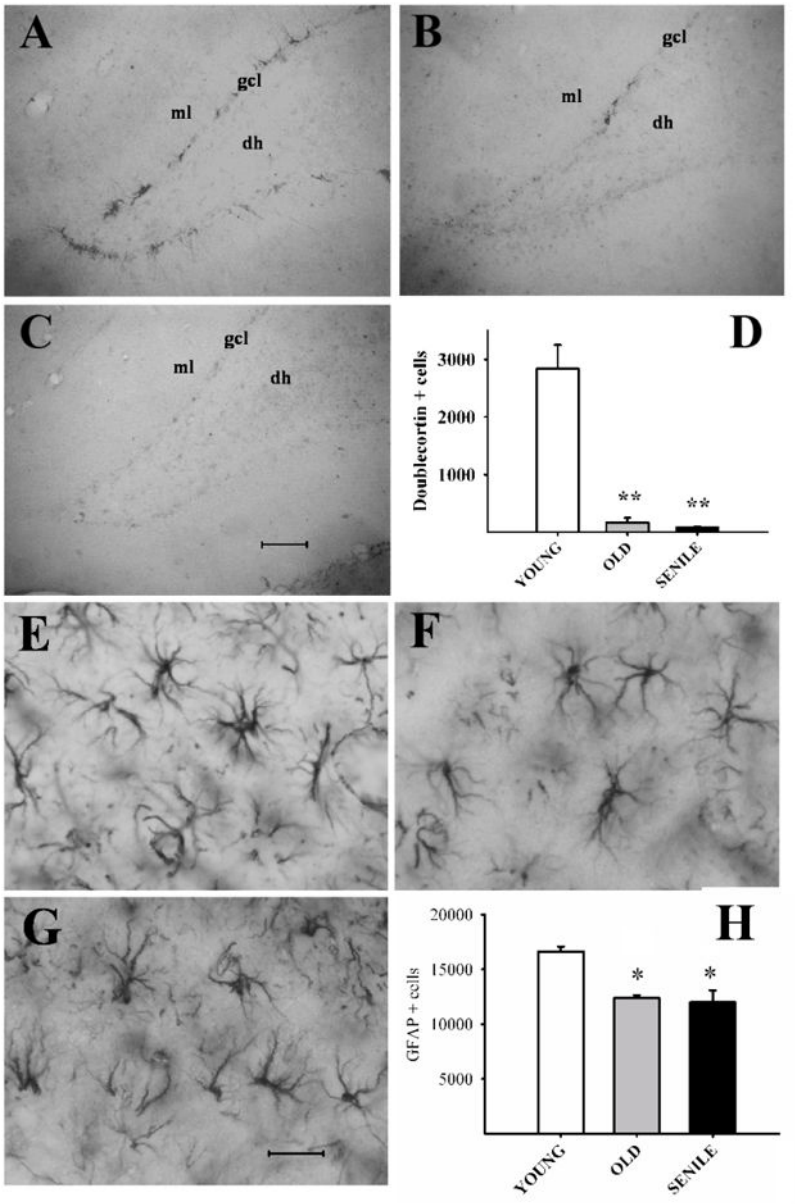

Figure 7. Doublecortin (DCX) and glial fibrillary acidic protein (GFAP) expression in the dorsal hippocampus of young, old and senile rats

Images: Coronal sections of the dentate gyrus in representative animals of each age group showing DCX(+) neurons (Panels A–C) and of the stratum radiatum for GFAP (+) cells (Panels E–G). Scale bars: 100 μm for DCX images and 25 μm for GFAP. DCX and GFAP cell numbers are plotted in Panel D and H, respectively. Note the sharp age related fall in DCX cell numbers. Abbreviations: dh (dentate hilus); gcl (granular cell layer); ml (molecular layer). Number of young, old and senescent hippocampi assessed for DCX was 6 for the 3 age groups and was 5, 6 and 5, respectively for GFAP. Other details are as in Fig. 2. The Holm-Sidak post hoc test was used for group comparisons in both plots.

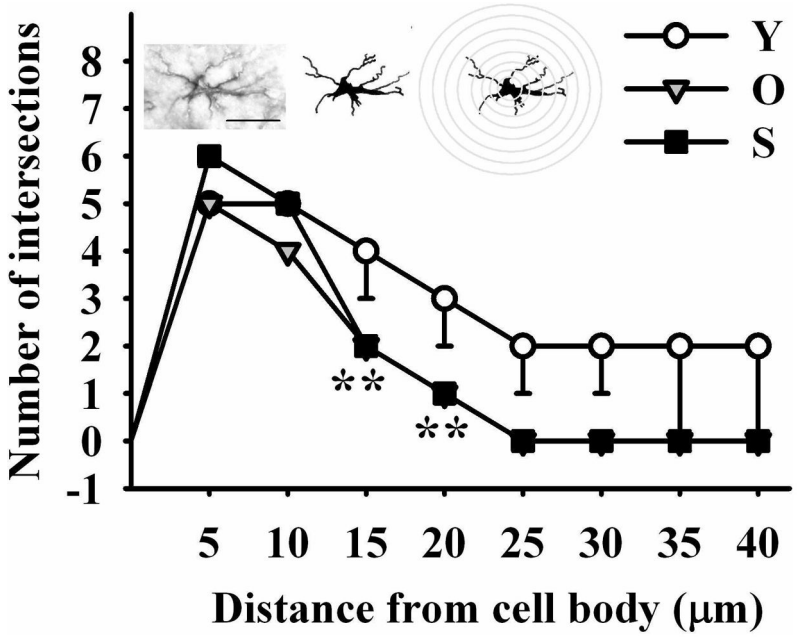

Figure 8. Impact of age on the length and complexity of glial processes in the stratum radiatum

Astroglial process numbers and length were drawn on a printed image, scaled up and analyzed with NIH software ImageJ running the Sholl Analysis Plugin v1.0. As shown by the scheme over the graph, a grid with concentric rings or shells distributed at equal distances **d** centered on the soma of a cell was superimposed on GFAP immunoreactive astrocyte images. The number of process intersections **i** per shell was computed and branching complexity evaluated. The length of the processes was estimated by the sum of the products of **d** by **i** for each ring. Holm-Sidak post-hoc test; Double asterisks represent highly significant differences (P<001) of aged animals versus the corresponding young control for the indicated points. The number of hippocampi assessed was 3 for each age group. Scale bar: 20 μm.

Table 1

Target-seeking activity of young and aging rats

PROBE TRIAL 1				
AGE GROUP	**YOUNG**	**OLD**	**SENESCENT**	
Total activity (#of explorations)	6.9 ± 0.4 n=30	6.6 ± 0.5 n=19	4.1 ± 0.4 n=21	Y vs S $p<0.05$ Other NS
Explorations per hole	0.34 ± 0.02	0.33 ± 0.03	0.20 ± 0.02	Y vs S $p<0.05$ Other NS
% versus Young	100 %	96 %	59 %	
Δ %	-	4	41	

PROBE TRIAL 2				
AGE GROUP	**YOUNG**	**OLD**	**SENESCENT**	
Total activity (#of explorations)	6.1 ± 0.4 n=29	5.1 ± 0.5 n=20	3.6 ± 0.4 n=24	Y vs S $p<0.05$ Other NS
Explorations per hole	0.30 ± 0.02	0.26 ± 0.03	0.18 ± 0.02	Y vs S $p<0.05$ Other NS
% versus Young	100 %	84 %	59 %	
Δ %	-	13	41	

Table 2

Mean volume of stratum radiatum and hilus and neuron number in the CA1 region of young, old and senile female rats

	Young	Old	Senile
SR volume (One-way ANOVA: F_2=0.343; p=0.658)	1.99 ± 0.13 mm^3(n=3)	1.92 ± 0.03 mm^3(n=3)	1.73 ± 0.16 mm^3(n=3)
Hilus volume (One-way ANOVA: F_2=3.069; p=0.135)	0.52 ± 0.03 mm^3(n=2)	0.50 ± 0.02 mm^3(n=3)	0.54 ± 0.02 mm^3(n=3)
Neuron number in CA1 **(One-way ANOVA: F_2=0.449; p=0.658)**	84547± 4454 (n=3)	94544± 11986 (n=3)	93697± 6472 (n=3)